Original article

Development of a coastal upwelling front driven by advection and topographic effects in the North Sea–Baltic Sea transition

Création d'une remontée côtière par advection due au vent et effet topographique à la frontière entre la mer du Nord et la Baltique

Lars Chresten Lund-Hansen [a,*], Torben Vang [b]

[a] Department of Marine Sciences, Institute of Biological Sciences, Aarhus University, Finlandsgade 12, 8200 Aarhus N, Denmark
[b] Vejle County, Coastal Section, Damhaven 12, 7100 Vejle, Denmark

Abstract

Upwelling of cold, saline, and nutrient rich water was observed in late September 1999 along an east–west transect in the SW Kattegat. The Kattegat forms part of the transitional zone between the high saline North Sea and the low saline Baltic Sea. The upwelling occurred after an extended period of northward flow and eastern winds in the Kattegat, that changed into a southward flow as wind ceased. The upwelling was the result of a combination of high current speeds and bottom topography whereby the high-speed inflow water was forced towards the surface at the slope. Nutrient data show that the upwelling brought nutrient rich bottom water to the light exposed surface and a related strong (1943.5 ml^{-1}) bloom of *Pseudo-nitzschia pseudodelicatissima* was observed. Surface (1.0 m) chlorophyll-*a* values increased from 3.7 to 10.0 µg l^{-1} during upwelling. A frontal structure developed during the upwelling with raised fluorescence values at the front related to convergence. The present upwelling front was only indirectly related to the wind conditions and the front propagated off shore as compared to other upwelling fronts.
© 2003 Éditions scientifiques et médicales Elsevier SAS and Ifremer/CNRS/IRD. All rights reserved.

Résumé

Un upwelling d'eau froide riche en nutriments a été observé fin septembre 1999 le long d'une section d'est en ouest au sud-ouest du Kattegat. Le Kattegat fait partie de la zone de transition entre la mer du Nord, de forte salinité, et la mer Baltique, de faible salinité. L'upwelling se produit après une longue période de courant de nord et de vents d'est dans le Kattegat, ce qui génère un courant de sud lorsque le vent cesse. L'upwelling est le résultat d'une combinaison de forts courants et d'une topographie du fond qui permet la remontée de l'eau vers la surface au niveau de la pente. Les résultats montrent que la remontée d'eau riche en nutriments vers la surface exposée à la lumière permet une floraison de *Pseudo-nitzschia pseudodelicatissima*. La teneur en chlorophylle *a* en surface de 3.7 à 10.0 g l^{-1} pendant l'upwelling. Une structure se développe au front de l'upwelling avec des valeurs élevées de fluorescence en relation avec la convergence. L'upwelling actuel est seulement indirectement corrélé au vent et le front se propage au large comme dans le cas des autres fronts d'upwelling.
© 2003 Éditions scientifiques et médicales Elsevier SAS and Ifremer/CNRS/IRD. All rights reserved.

1. Introduction

Upwelling occurs on a variety of time and spatial scales, spanning from the extensive (~5000 km) and persistent up-welling areas along the Chilean coast (Peterson et al., 1988; Shaffer, 1988; Djurfeldt, 1994; Shaffer et al., 1999; Blanco et al., 2001; Morales et al., 2001) to the more episodic and small-scale (~50 km) upwellings at the northern Iberian coast (Blanton et al., 1984; Hanson et al., 1986; Roson et al., 1997; Álvarez-Salgado et al., 2000). Upwelling is generally related

* Corresponding author.
E-mail address: lund-hansen@biology.au.dk (L.C. Lund-Hansen).

to wind induced Ekman transport whereby cold and nutrient rich bottom and subsurface waters enter the photic zone leading to enhanced primary production (Mann and Lazier, 1996). However, less attention has been paid to the frontal systems that under certain conditions develop in upwelling regions. A conceptual model study showed that an upwelling front might be established where a strong geostrophic flow at the outer shelf is balanced with the Ekman transport (Mooers et al., 1978). A recent coastal field study, based on both CTD transects and continuous CTD profiling at an anchor station at Duck, North Carolina, showed that a frontal system developed and propagated shorewards as the upwelling generating winds ceased (Shanks et al., 2000). Strong convergence occurred on both sides of the front whereby planktonic larvae were concentrated at the front and transported shorewards, which establish a potentially important larvae cross-shelf transport mechanism.

The present study describes in detail a coastal upwelling front, which developed during a period of enhanced water flow from the Skagerrak/Kattegat towards the Baltic Sea. The upwelling was related to a strong inflow of saline water and topographic effects whereby the water was forced towards the surface at more shallow water. Nutrient concentrations were high in the inflow water and high fluorescence values were observed at the front due to convergence and blooming.

It has earlier been shown that bathymetric features may enhance wind driven upwelling, for instance in some Spanish rias (Blanton et al., 1984; Roson et al., 1997; Álvarez-Salgado et al., 2000).

2. Study area, methods and data

The study area is the waters north of Funen in the southwest Kattegat, a part of the transitional zone between the high saline North Sea and the low saline Baltic Sea, confined by two major hydraulic boundaries with the Little Belt in the southwest and the Great Belt in the east (Fig. 1). Profiles of salinity, temperature, and fluorescence were obtained with a CTD (GMI—Geological and Marine Instrumentations, Denmark) with a vertical resolution of 0.2 m. The Scan Fish (GMI), a towed CTD that automatically undulates between the surface and bottom in the sailing direction continuously recording variables, was applied during two cruises and tracks are shown in Fig. 1. The Scan Fish descend velocity varied between 0.5 and 1 m s^{-1} in order to obtain nearly equidistant data points, whereas ascend velocity was between 5 and 10 m s^{-1}. Horizontal resolution was about one CTD profile per 2 km and the vertical resolution about 0.4–0.5 m. Water samples for nutrient analyses and chlorophyll-*a* were collected with Niskin bottles at 5, 15, and
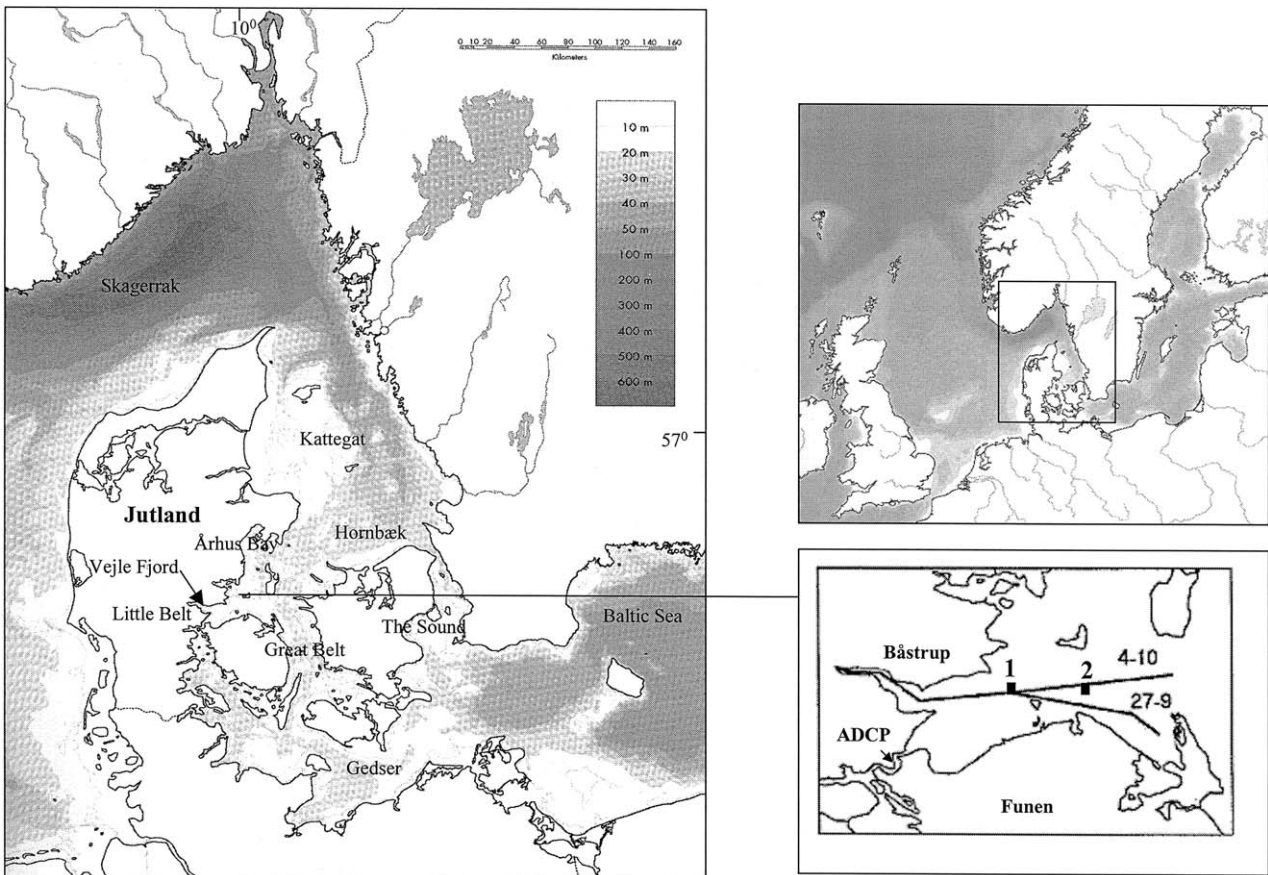

Fig. 1. Study area.

19 m of water depth at position 1. Nutrient analyses were carried out following standard procedures (Grasshoff et al., 1983) and chlorophyll-*a* content was determined following Lorenzen (1967). Samples for phytoplankton species composition were collected with a standard 20 μm phytoplankton net also at position 1. Species composition was determined by normal light microscopy whereas electron-scanning microscope was used to identify the diatoms belonging to the group of *Pseudo-nitzschia*. Data on current conditions were obtained from the bottom mounted ADCP in both the Little Belt (RDI Workhorse) with a vertical resolution of 1 m (40 m), and the Great Belt (Aanderaa RCM 11). The Great Belt current meter was placed in the central part of the belt. Data on wind conditions were obtained from Båstrup about 8 km north of Vejle Fjord (Fig. 1).

3. Results and discussion

The Kattegat and Skagerrak areas were dominated by eastern winds between 1 and 20 September with average and maximum wind speeds of 6.2 and 13.4 m s^{-1}, respectively. Water level was on average 17 cm higher in the southwest Baltic Sea relative to the Kattegat during this period with a maximum of 56 cm on 20 September (not shown). The difference in water level between Gedser (southwest Baltic Sea) and Hornbæk (Kattegat) (Fig. 1) is used as a general indicator of the water flow direction through inner Danish waters, where a higher water level at Gedser relative to Hornbæk indicates a water flow towards the Kattegat from the Baltic Sea and vice versa (Stigebrandt, 1983; Møller, 1996; Gustafsson, 2000). However, wind direction changed to southwest around 21 September, which prevailed between 22 and 30 September at an average speed of 6 m s^{-1} and a maximum of 12 m s^{-1} (Fig. 2A). Average water level difference between Gedser and Hornbæk is negative (–19 cm) during this period where negative values designate a flow towards the Baltic Sea. The change in wind direction and reversal of the current in the Great Belt is clearly seen around 21–22 September (Fig. 2A,B). Current direction changed also into southward in the Little Belt region around 22 September as seen from the vertically integrated ADCP current data where a negative value is into Little Belt from the Kattegat and opposite (Fig. 2). Current speed was resolved into northwest and southeast directions, which are the flow directions in the central Little Belt at the ADCP position (Fig. 1). However, the dominant flow into the Little Belt prevails until 5–6 October (Fig. 2C).

3.1. Upwelling and driving forces

A Scan Fish survey was carried out on 27 September covering a distance of 64 km from the inner part of Vejle Fjord across the study area (Fig. 1). Water depths were automatically recorded along the track but note that the 4 m of water depths at 4 km from Vejle Port were recorded when the ship left the navigational channel (Fig. 3A). However,

salinity isopleth shows a strong horizontal gradient with maximum surface salinities of 27 in the western (left) part of the transect and comparatively low (19–21) salinities in the eastern (Fig. 3A). Secondly, the salinity interface around the 25 isohaline inclines towards the east (0.15 m km^{-1}) and reaches into the surface at about 14 km where surface salinity is high (27–29). This shows clearly that upwelling occurs in the western part where the high saline water reaches into the surface, and temperature of the upwelling saline water was lower (13.0–14.5 °C) as compared to the temperature of the surface (15.5–1 °C) water in the eastern part of the transect. A comparison of CTD-casts from position 1 shows that the major salinity changes occurred at mid-depths between pre-inflow (22 September) and upwelling (30 September) (Fig. 4). For instance, salinity increased by 8.2 at 12 m of water depth between pre-inflow and upwelling, whereas salinity only increased by 0.8 at 20 m. The inflow at mid-depths is further demonstrated by the rise of the interface from about 12 m on 22 September (Fig. 4A) to about 6 m of water depth on 30 September (Fig. 4B). The nearly horizontal 31 isohaline during upwelling indicates additionally that the water mass in the topographic depression was not affected by the upwelling in the initial stage (Fig. 3A). These data indicate that the upwelling was the result of an inflow of saline water from the Kattegat area related to the change in current direction in the Little and Great Belt (Fig. 3B,C). However, the upwelling could as well be related to local Ekman transport but the calculated internal Rossby radius of deformation (R_i) was only about 5 km, which is a factor two lower than the observed radius of 10–12 km (Fig. 3A). The internal Rossby radius of deformation (R_i) is given by

$$R_i = \frac{(g'H)^{(1/2)}}{f} \qquad (1)$$

where g' is the reduced gravity (m s^{-2}), H the depth of the upper layer (m), and f the Coriolis parameter (s^{-1}) (Mann and Lazier, 1996). That the upwelling was not driven by Ekman transport is further supported by the fact that wind speed, on average, only reached 3.7 m s^{-1} from the southwest direction between 22 and 27 September (Fig. 2A). Another upwelling mechanism is provided by the offshore winds where halocline inclination would reach about 0.014 m km^{-1} based on observed wind speed, water density, and basin geometry, following Pedersen (1986). This is, however, about 10 times less than the observed inclination (Fig. 3A), although wind driven upwelling in the area has been observed in the periods of strong offshore western winds (Christiansen et al., 1997; Lund-Hansen et al., 1996, 1997). It is thus strongly supposed that the upwelling occurred as a combination of high current speeds in the inflow water and topographic effects whereby this water was forced towards the surface. For instance, current speed reached up to 1.0 m s^{-1} in the Great Belt during 27 September and average current speed in the Little Belt reached a maximum of about 1.30 m s^{-1} on the same day (Fig. 2B,C). Bottom topography along the transect forms a gentle slope where water depth slightly decreases in the

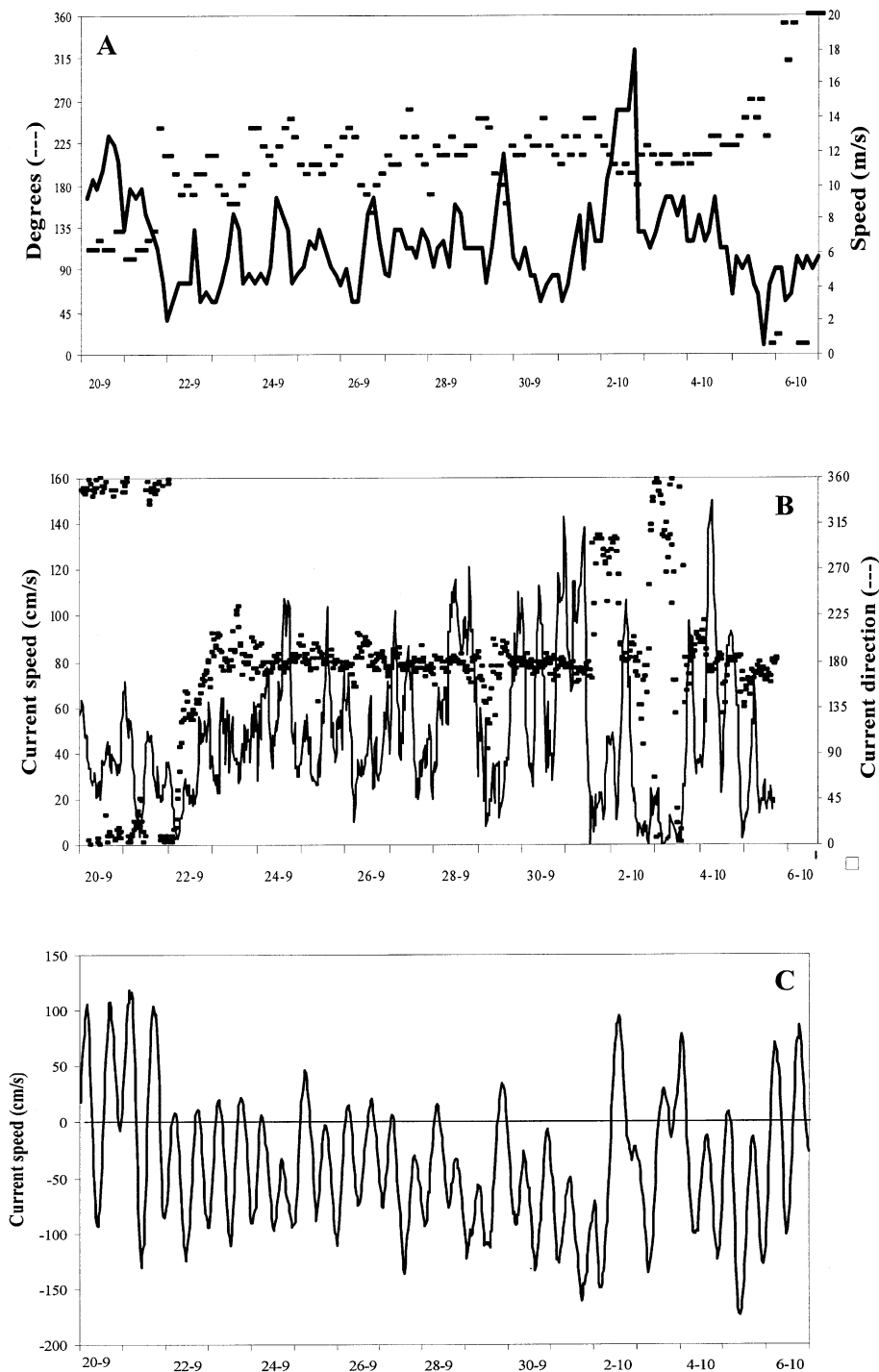Fig. 2. (A) Wind speed (m s^{-1}) (full line) and direction (°) at Båstrup. (B) Current speed (cm s^{-1}) (—) and direction (°) (■■■) in the Great Belt at 7.6 m of water depth. (C) Northwest–southeast projected depth averaged ADCP current speed (cm s^{-1}) in the Little Belt between 20 September and 6 October 1999. Negative values designate water flow into the Little Belt and positive values water flow out of the Little Belt.

western part of the transect (Fig. 3). It has been shown in several studies that the wind driven upwelling was enhanced by topographic features, as observed in dimensionally similar rias (Blanton et al., 1984; Roson et al., 1997), and shown by models at the New Jersey coast (Song et al., 2001). It has further been shown in a numerical study of the Eastern Australia upwelling that an along shore shelf current in combination with a gently sloping shelf were the driving

mechanisms in the coastal upwelling (Oke and Middlelton, 1999).

3.2. Frontal structure

The inflow and upwelling of the high saline (27–29) water displaced the interface between the surface and the bottom water upwards whereby a frontal structure was established,
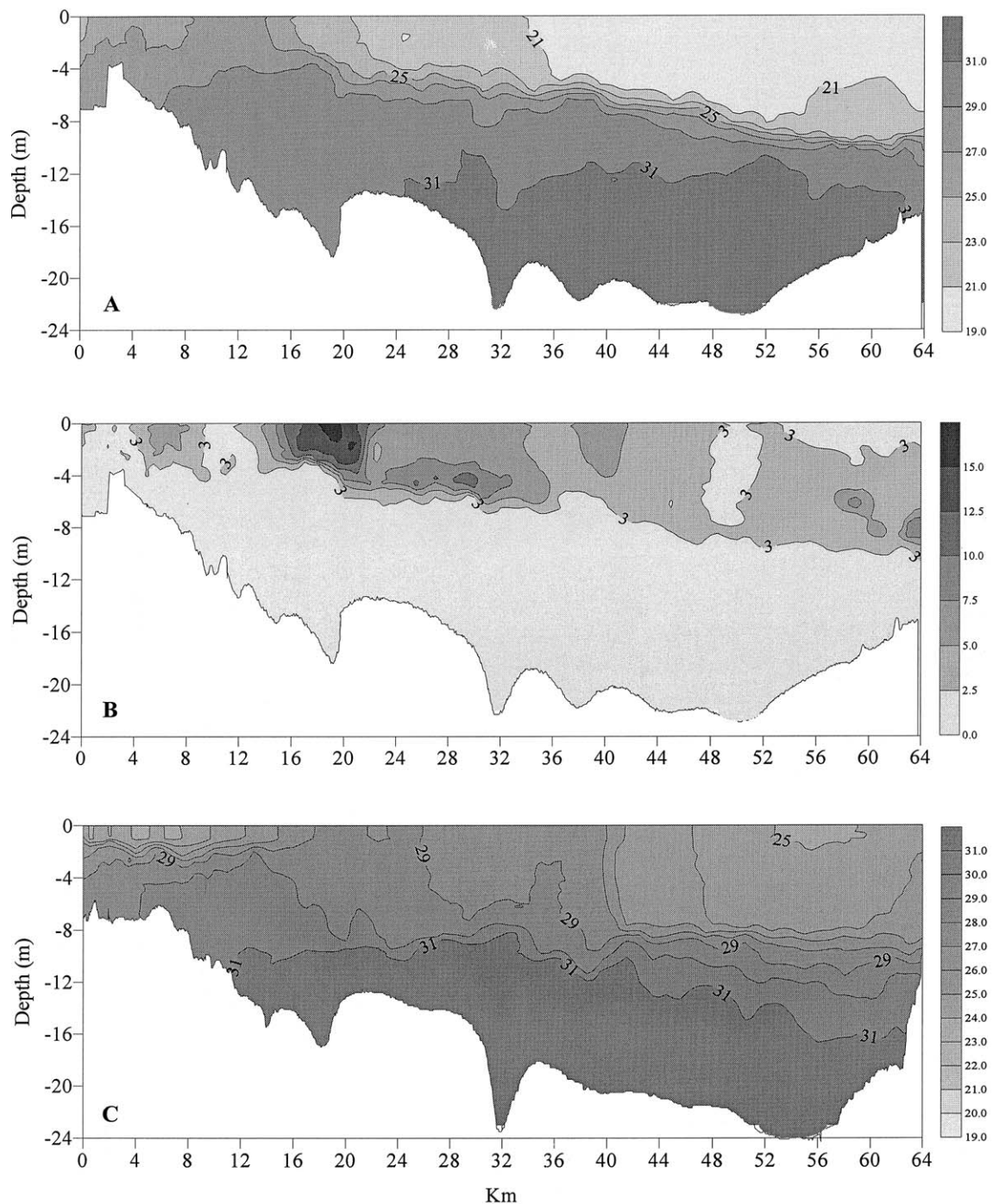
Fig. 3. (A) Salinity and (B) fluorescence (arbitrary units) isopleths — measured 27 September. (C) Salinity isopleth — measured 4 October.

i.e. marked changes in selected parameters within a comparatively short horizontal distance (Simpson and James, 1986). The frontal structure is here recognised as a high surface salinity gradient (~1 km^{-1}) at about 16 km from Vejle Fjord (Fig. 3A). A surface temperature gradient of about 0.17 °C km^{-1} was similarly observed in the front, which is a high gradient as compared to the thermal fronts in the Celtic (~0.027 °C km^{-1}) (James, 1977) and Irish Sea's (~0.125 °C km^{-1}) (Richardson et al., 1985). Fluorescence isopleth shows that fluorescence is highly variable (2.5–17.5) in the surface

layer (0–10 m) and that the maximum fluorescence patch (7.5– 17.5) is located in the front along with the maximum salinity and temperature gradients (Fig. 3A,B). This fluorescence patch is in extent and distribution very similar to the patches of raised chlorophyll-*a* levels observed at the Ushant front (Pingree et al., 1975) and in the Irish Sea (Richardson et al., 1985). These high chlorophyll-*a* patches were supposedly related to the convergence, which tends to accumulate phytoplankton where the more dense water sinks below the warm surface water (Pingree et al., 1975). High
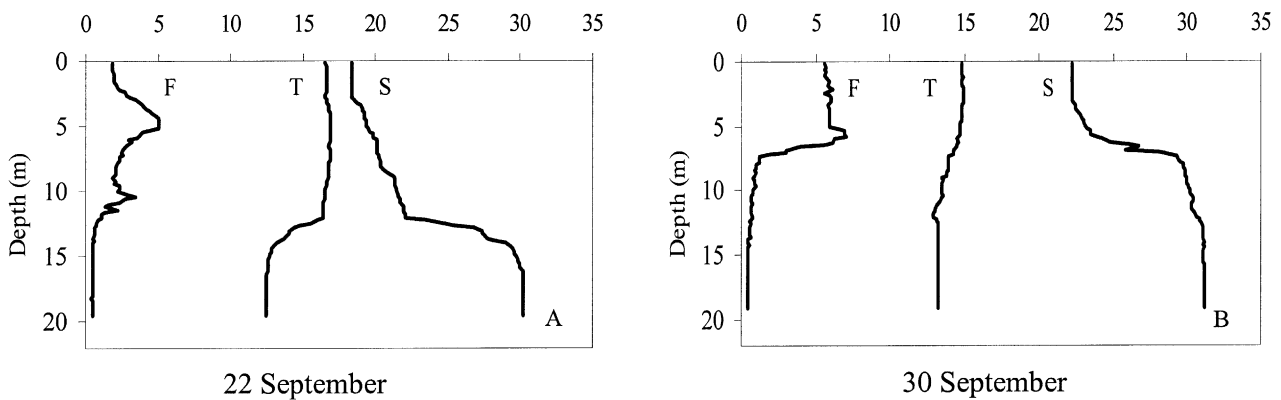
Fig. 4. Profiles of salinity (*S*), temperature (°C) (*T*), and fluorescence (arbitrary values) (*F*) — (A) Position 1 on 22 September, and (B) position 1 on 30 September.

chlorophyll-*a* regions occur generally on the stratified side of the front (Simpson and James, 1986), which is also the case in the present study, indirectly shown by the high fluorescence level at the front (Fig. 3A,B). However, the inflow and upwelling caused an offshore movement of the surface layer in the present study whereby convergence was established in the front, and it is strongly supposed that the maximum fluorescence patch (7.5–17.5) was related to the convergence processes. This is further substantiated by the raised but lower fluorescence values (5.0–10.0) outside the frontal region confined to the 21–23 interval (Fig. 3A,B). However, the raised (5.0–10.0) fluorescence values strongly indicate, as compared to the background values (0.0–5.0) in the 19–21 surface, that a phytoplankton surface bloom developed along with the upwelling (see later). Convergence zones were also generated at the Shanks et al. (2000) upwelling front, although that it was larvae found in high concentrations and not fluorescence. Fronts in the central Kattegat, which develop in the region where northward flowing Great Belt water interfere with water from the Sound (Fig. 1) have earlier been described (Pedersen, 1993), whereas the present study is the first description of an upwelling front in the low tidal North Sea–Baltic Sea transition.

3.3. Chlorophyll, fluorescence, and nutrients

Chlorophyll-*a* concentrations increased from 3.7 to 10.0 µg l^{-1} in the surface (1.0 m) layer at position 1 between 14 and 28 September, which is before and during the upwelling. A parallel increase in depth-averaged fluorescence from 2.7 to 5.1 in the surface layer occurred between 22 and 30 September at the same position (Fig. 4). There were only slight changes in the nutrient concentrations at position 1 before and during the upwelling except for bottom water silicate concentrations that were halved (Fig. 5). However, nutrient concentrations are on average a factor 4.5 higher in the bottom water (15–19 m) compared to the surface waters (5 m) before the upwelling (14 September). This shows in combination with chlorophyll-*a* and fluorescence data that the upwelling transported nutrient rich water into the surface, whereby fluorescence level and thus chlorophyll-*a* concentrations increased due to the enhanced phytoplankton growth
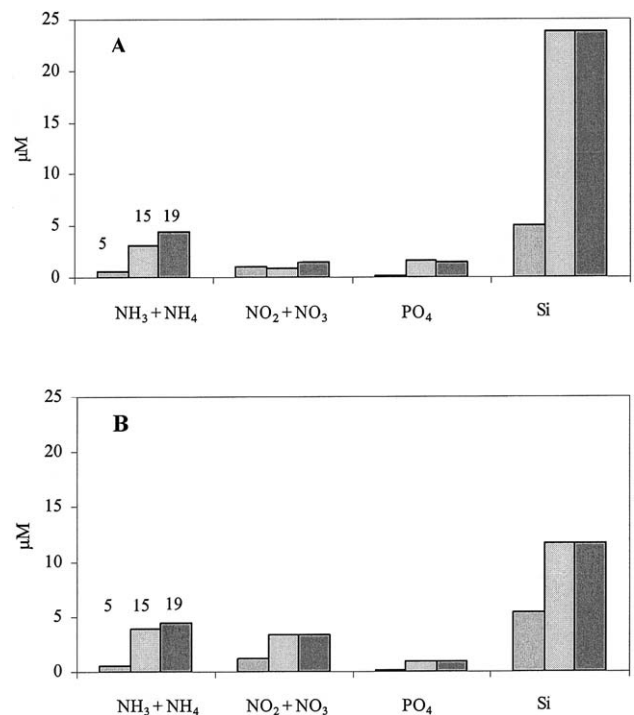

Fig. 5. Nutrient concentrations (µM) at position 1 at depths (5, 15 and 19 m) on 14 (A) and 28 (B) September.

in the light exposed part of the water column. The rise in chlorophyll-*a* and fluorescence is further substantiated by the fact that the diatom *Pseudo-nitzschia pseudodelicatissima*, which belong to a potential toxic group (Bates et al., 1989), was present in a high (1943.5 ml^{-1}) number at position 1 on 28 September. This species was not present on 9 September, whereas *Gymnodinium chloroforum*, another dominant species, was present (~120 ml^{-1}) during both the sampling dates. However, there is a 19 d lapse between phytoplankton sampling dates, but data strongly indicate that the corresponding chlorophyll-*a* and fluorescence increase was related to a bloom of *Pseudo-nitzschia pseudodelicatissima*. Nevertheless, fluorescence remained low (0–2.5) and constant in the high (27–29) saline water that reached into the surface around 12 km in the upwelling zone (Fig. 3A,B). Oxygen

concentrations were low (2.0–4.0 mg l^{-1}) in the bottom water below 27 and the absence of a raised fluorescence level in these waters might be related to the low oxygen concentrations. An inflow related oxygen reduction in the study has earlier been described and was related to the wind driven inflow (Skyum et al., 1994).

3.4. Post upwelling

A second Scan Fish survey was conducted during 4 October along the 27 September track except that the eastern part of the track was displaced northwards (Fig. 1). Salinity isopleth shows that a frontal structure is still present where the 26–28 isohalines reach into the surface and that the front was displaced about 25 km eastward, as compared to 4 October (Fig. 3A–C). The high (31) saline bottom water extends towards the entrance of the Vejle Fjord. The eastward displacement of the surface front and the extended inflow of high saline water strongly indicate, that the upwelling was maintained between 27 September and 4 October. The regions of high fluorescence levels at the front as during 27 September are on 4 October replaced by an even and uniform fluorescence level (4–8) confined by the 29 isohaline in the eastern part (Fig. 3C), whereas fluorescence level is low (0–4) in the western part of the track (not shown). This indicates that the convergence was only active during the initial stage of the upwelling whereby the high fluorescence levels at the front developed. However, the southward directed flow ceased around 5–6 October, where dominant current direction changed to northwards in the Little Belt (Fig. 2C). It is anticipated that the upwelling ceased around 5–6 October when southward current direction was less dominant in the Little Belt. This gives an overall upwelling period of 7–8 d, which is similar to the upwelling periods observed in Spanish rias (Hanson et al., 1986; Roson et al., 1997; Álvarez-Salgado et al., 2000).

4. Conclusions

The upwelling was established by a southward flow in the North Sea–Baltic Sea transition as the persistent eastern winds that promote northwards flow in the transition ceased. The southward flow was barotropic forced, as the water level was higher in the Kattegat north of the study area as compared to the Baltic Sea. The inflow of water in the study area occurred around mid-depths near the main interface. The inflow water was forced towards the surface as it reached the bottom slope outside Vejle Fjord whereby the upwelling was established. The inflow and upwelling brought nutrient rich water into the photic zone, which resulted in an extended bloom of the diatom *Pseudo-nitzschia pseudodelicatissima*. A frontal system of strong salinity and temperature gradients developed in relation to the upwelling set up the convergence. However, the observed upwelling front differs from others in that the upwelling was only indirectly related to the wind conditions and as the upwelling front propagated off shore.

References

Álvarez-Salgado,, X.A., Gago, J., Míguez, B.M., Gilcoto, M., Pérez, F.F., 2000. Surface waters of the NW Iberian margin: upwelling on the shelf versus outwelling of the upwelled waters from the Rias Baixas. Est. Coast. Shelf Sci. 51, 821–837.

Bates, S.S., Bird, C.J., Freitas, A.S.W., Foxall, R., Gilgan, M.W., Hanic, L.A., Johnson, G.E., McCulloch, A.W., Pocklington, R., Quilliam, M.A., Sim, P.G., Smith, J.C., Subba, R.D.V., Todd, E.D.C., Walter, J.A., Wright, J.L.C., 1989. Pennate diatom Nitzschia pungens as the primary source of domoic acid, a toxin in shellfish from Eastern Prince Edward Islands, Canada. Can. J. Fish. Aq. Sci. 46, 1203–1215.

Blanton, J.O., Atkinson, L.P., Castillejo, F.F., Montero, A.L., 1984. Coastal upwelling off the Rias Bajas, Galicia, northwest Spain I: hydrographic studies. Rapp. P.-v. Réun. Cons. Int. Explor. Mer. 183, 79–90.

Blanco, J.L., Thomas, A.C., Carr, M.-E., Strub, P.T., 2001. Seasonal climatology of hydrographic conditions in the upwelling region off northern Chile. J. Geophys. Res. 106 (C6), 11451–11467.

Christiansen, C., Gertz, F., Laima, M.J.C., Lund-Hansen, L.C., Vang, T., Jürgensen, C., 1997. Nutrient (P, N) dynamics in the southwestern Kattegat, Scandinavia: sedimentation and resuspension effects. Environ. Geol. 29, 66–77.

Djurfeldt, L., 1994. The influence of physical factors on a subsurface chlorophyll maximum in an upwelling area. Est. Coast. Shelf Sci. 39, 389–400.

Grasshoff, K., Erhardt, M., Kremlin, K., 1983. Methods of Seawater Analyses. Verlag Chemie, Weinheim.

Gustafsson, B.G., 2000. Time-dependent modelling of the Baltic entrance area. 1. Quantification of circulation and residence times in the Kattegat and the straits of the Baltic sill. Estuaries 23, 231–252.

Hanson, R.B., Alvarez-O, M.T., Cal, R., Campos, M.J., Roman, M., Santiago, G., Varela, M., Yoder, J.A., 1986. Plankton response following a spring upwelling event in the Ria de Arosa, Spain. Mar. Ecol. Prog. Ser. 32, 101–113.

James, I.D., 1977. A model of the annual cycle of temperature in a frontal region of the Celtic Sea. Est. Coast Mar. Sci. 5, 339–353.

Lorenzen, C.J., 1967. Vertical distribution of chlorophyll and phaeopigments: Baja California. Deep-Sea Res. 14, 735–745.

Lund-Hansen, L.C., Skyum, P., Christiansen, C., 1996. Modes of stratification in a semi-enclosed bay at the North Sea–Baltic Sea transition. Est. Coast. Shelf Sci. 42, 45–54.

Lund-Hansen, L.C., Christiansen, C., Vang, T., Laima, M., 1997. Regional North Sea–Baltic Sea circulation impact on local Kattegat fjords and bays. Aarhus Geosci. 7, 21–33.

Mann, K.H., Lazier, J.R.N., 1996. Dynamics of Marine Ecosystems. Biological–Physical Interactions in the Ocean. Blackwell Science.

Mooers, C.N.K., Flagg, C.N., Boicourt, W.C., 1978. Prograde and retrograde fronts. In: Bowman, J.M., Esaias, W.E. (Eds.), Oceanic Fronts in Coastal Processes, vols. 43–58. Springer-Verlag, New York 114 p.

Morales, C.E., Blanco, J.L., Braun, M., Silva, N., 2001. Chlorophyll-a distribution and mesoscale physical processes in upwelling and adjacent oceanic zones off northern Chile (summer–autumn 1994). J. Mar. Biol. Ass. UK 81, 193–206.

Møller, J.S., 1996. Water masses, stratification and circulation. Eutrophication in Coastal Marine Ecosystems. In: Jørgensen, B.B., Richardson, K. (Eds.), Coastal and Estuarine Studies. American Geophysical Union 52.

Peterson, W.T., Arcos, D.F., McManus, G.B., Dam, H., Bellantoni, D., Johnson, T., Tiselius, P., 1988. The nearshore zone during coastal upwelling: Daily variability and coupling between primary and secondary production of central Chile. Prog. Oceangr. 20, 1–40.

Pedersen, F.B., 1986. Environmental Hydraulics: Stratified Flows. Lecture Notes on Coastal and Estuarine Studies, vol. 18. Springer-Verlag, Berlin 278 p.

Pedersen, F.B., 1993. Fronts in the Kattegat: the hydrodynamic regulating factor for biology. Estuaries 16, 104–112.

Pingree, R.D., Pugh, P.R., Holligan, P.M., Forster, G.R., 1975. Summer phytoplankton blooms and red tides along tidal fronts in the approaches to the English Channel. Nature (London) 258, 672–677.

Oke, P.R., Middleton, J.H., 1999. Topographically induced upwelling off Eastern Australia. J. Phys. Oceanogr. 30, 512–531.

Roson, G., Álvarez-Salgado,, X.A., Pérez, F.F., 1997. A non-stationary box model to determine residual fluxes in a partially mixed estuary, based on both thermohaline properties: application to the Ria de Arousa (NW Spain). Est. Coast. Shelf Sci. 44, 249–262.

Richardson, K.R., Peregrina-L, M.F., Mitchelson, E.G., Simpson, J.H., 1985. Seasonal distribution of chlorophyll-*a* in relation to the physical structure in the western Irish Sea. Oceanol. Acta 8, 77–86.

Shaffer, G., 1988. On the upwelling circulation over the wide shelf off Peru: 1. Circulation. J. Mar. Res. 40, 293–314.

Shaffer, G., Hormazábal, S.E., Pizzaro, O., Salinas, S., 1999. Seasonal and interannual variability of current and temperature off Central Chile. J. Geophys. Res. 104, 29951–29961.

Shanks, A.L., Largier, J., Brink, L., 2000. Demonstration of the onshore transport of larval invertebrates by the shoreward movement of an upwelling front. Limnol. Oceanogr. 45, 230–236.

Simpson, J.H., James, I.D., 1986. Coastal and estuarine fronts. In: Mooers, C.N.K (Ed.), Baroclinic Processes on the Continental Shelves, 3. American Geophysical Union, Coast. Est. Sci, Washingtin (DC), pp. 63–93.

Skyum, P., Christiansen, C., Lund-Hansen, L.C., Nielsen, J., 1994. Advection induced changes in oxygen variability in the North Sea–Baltic Sea transition. Hydrobiology 281, 65–77.

Song, Y.T., Haidvogel, D.B., Glenn, S.M., 2001. Effects of topographic variability of upwelling centers off New Jersey: a theoretical model. J. Geophys. Res. 106, 9223–9240.

Stigebrandt, A., 1983. A model for the exchange of water and salt between the Baltic and the Skagerrak. J. Phys. Oceanogr. 13, 411–427.